

## Publication II

U. Ehrnstén, M. Ivanchenko, V. Nevdacha, Y. Yagodzinsky, A. Toivonen, and H. Hänninen. 2005. Dynamic strain ageing and EAC of deformed nitrogen-alloyed AISI 316 stainless steels. In: Todd R. Allen, Peter J. King, and Lawrence Nelson (editors). Proceedings of the 12th International Conference on Environmental Degradation of Materials in Nuclear Power Systems – Water Reactors. Salt Lake City, Utah, USA. 14-18 August 2005. TMS. Pages 1475-1482. ISBN 1-604-23633-7.

© 2005 The Minerals, Metals & Materials Society (TMS)

Reprinted by permission of The Minerals, Metals & Materials Society.

## DYNAMIC STRAIN AGEING AND EAC OF DEFORMED NITROGEN-ALLOYED AISI 316 STAINLESS STEELS

U. Ehrnsten<sup>1</sup>, M. Ivanchenko<sup>2</sup>, V. Nevdacha<sup>2</sup>, Y. Yagodzinsky<sup>2</sup>, A. Toivonen<sup>1</sup> and H. Hänninen<sup>2</sup>

<sup>1</sup> VTT Industrial Systems, Kemistintie 3, P.O. Box 1704, FIN-02044 VTT, Finland, email: ulla.ehrnsten@vtt.fi

<sup>2</sup> Helsinki University of Technology, Department of Mechanical Engineering, Puumiehenkuja 3, P.O. Box 4200, FIN-02015 HUT, Finland

Keywords: Dynamic strain ageing, Stainless steels, Environmentally assisted cracking

### Abstract

Intergranular stress corrosion cracking has occurred in BWR environments in non-sensitised, cold-worked austenitic stainless steel materials. The affecting parameters are so far not fully known, but deformation mechanisms may be decisive. The effect of cold deformation and nitrogen content on the deformation behaviour of austenitic stainless steels was investigated. The materials were austenitic stainless steels of AISI 316L type with different amounts of nitrogen (0.03...0.18%) and they were deformed in tension 0, 5 and 20% before further investigations. The investigations were focused on the dynamic strain ageing (DSA) behaviour as a function of nitrogen level and deformation. A few crack growth rate measurements are performed on nuclear grade AISI 316NG stainless steel with different degrees of deformation (0, 5 and 20%). The effects of DSA on mechanical properties of these materials were evaluated based on peaks in tensile strength and minimum in ductility in the DSA temperature range. Also the strain rate sensitivity in the DSA temperature range was investigated. Internal friction measurements were performed in the temperature range of -100...600 °C for determining nitrogen interactions with other alloying elements and dislocations. The results show effects of nitrogen on the stainless steel deformation behaviour, i.e. clear indications of dynamic strain ageing: serrated yielding, negative strain rate sensitivity and changes in the internal friction behaviour as a function of nitrogen content and amount of deformation. The apparent activation energy calculated from the DSA serration occurrence map corresponds to that of nitrogen diffusion. Fully intergranular cracking was obtained in the 20% deformed, non-sensitised AISI 316NG stainless steel in simulated BWR-environment. The crack growth data and the mechanism are discussed based on the unstable plastic flow of the material.

### Introduction

Since the early 1970's numerous cases of intergranular stress corrosion cracking (IGSCC) have occurred in boiling water reactors (BWR) in AISI 304 type austenitic stainless steels. The root cause for the cracking is a combination of tensile stresses, an oxidising environment and a sensitised material. The remedial actions taken have involved all three major parameters, e.g. application of narrow-gap welding technique to reduce residual stresses, increase of the overall purity of the primary water, application of hydrogen or noble metal water chemistry as well as reducing the amount of carbon in the stainless steels to avoid sensitisation. Nitrogen is added to maintain the strength level of austenitic stainless steels with reduced carbon levels. The

remedial actions have been successful and the amount of cracking due to IGSCC has decreased remarkably. However, in the early 90's the first cases of intergranular (IG) stress corrosion cracking in non-sensitised, low carbon austenitic stainless steels of type AISI 316NG and AISI 304L were observed [1, 2]. Several cases have so far been observed both in the HAZ of the welds as well as in the base metals far away from any weld. Although all affecting parameters are so far not known, deformation seems to be a common parameter. Several open questions are still connected to this type of cracking, such as a possible difference in the behaviour between different types of austenitic stainless steels, the effect of chemical composition, the effect of cold work (amount and temperature), the influence of constraint during welding, etc.

The affecting deformation mechanisms involve dynamic strain ageing (DSA) and possibly also environmentally enhanced creep. Dynamic strain ageing occurs in alloys containing solute atoms, which can rapidly and strongly segregate to dislocations and lock them during straining. The maximum effect of DSA corresponds to such conditions, where the solute atoms can follow by diffusion the changes of the dislocation structure. DSA is manifested by negative strain rate sensitivity, and serrated yielding during straining at elevated temperatures and results often in a remarkable degradation of mechanical properties for a number of engineering alloys. DSA phenomenon leads to inhomogeneous plastic flow, which can affect crack initiation and propagation.

Austenitic stainless steels show DSA behaviour in a wide range of temperatures (~200 – 800 °C) depending on the actual strain rate. Interstitial carbon and nitrogen atoms dissolved in the crystal lattice play a determining role in DSA of austenitic stainless steels in the temperature range between 200 °C and about 600 °C [3 - 5]. At higher temperatures, interaction between substitutional atoms, e.g. chromium and dislocations becomes decisive. Literature results have, however, also shown that nitrogen alloying shifts the onset temperature of DSA to higher values [6]. The aim of the present investigation was to study the effects of nitrogen alloying and deformation on DSA phenomenon in austenitic AISI 316L stainless steel at ~300 °C. The effect of deformation of AISI 316NG stainless steel on the cracking behaviour in BWR water was additionally investigated using rising and constant displacement loading.

### Experimental

Three model, type AISI 316L stainless steel plate materials with different nitrogen contents, but similar carbon contents, and a commercial nuclear grade AISI 316NG stainless steel pipe section

Table I. Chemical compositions of the studied stainless steels in weight %.

Type	Code	C	Si	Mn	P	S	Cr	Ni	Mo	Cu	Al	O <sub>2</sub>	N <sub>2</sub>
AISI 316L	1042	0.022	0.51	1.47	0.026	0.002	16.8	11.0	2.1	0.20	0.02	0.004	0.028
AISI 316L	1043	0.022	0.52	1.50	0.027	0.002	16.8	11.1	2.0	0.19	0.02	0.004	0.085
AISI 316L	1045	0.022	0.53	1.53	0.027	0.002	17.0	11.2	2.1	0.18	0.02	0.005	0.176
AISI 316NG	BB44	0.022	0.38	1.66	0.027	0.002	17.0	12.5	2.28	0.11	0.01	0.007	0.093
AISI 304	165	0.042	0.47	0.88	0.026	0.018	18.2	10.2					

were used in the study. A sensitised AISI 304 stainless steel pipe section was additionally used in the crack growth rate tests. The chemical compositions of the materials are shown in Table I. Details concerning the manufacturing of the model materials can be found in [7, 8]. The effect of deformation was investigated by pre-straining the materials at room temperature in tension before preparation of test specimens.

The microstructure and hardness (HV 10) of all AISI 316L materials were determined. The blanks for the tensile test specimens were cut from the plates, transverse to their rolling direction, and in the longitudinal direction from the AISI 316NG stainless steel pipe. All tensile test specimens were prepared according to ASTM standard E8M (sheet-type sub-size specimens). Tensile tests were performed according to the standards SFS-EN 1002-1 and ASTM E21 (Standard Test Method for Elevated Temperature Tension Tests of Metallic Materials) in air environment. Tensile tests for observing DSA were carried out using a 25 kN MTS 858 test machine equipped with a MTS High-Temperature Furnace 653.02 at strain rates of  $1 \times 10^{-4}$ ,  $1 \times 10^{-5}$ ,  $5 \times 10^{-6}$  and  $1 \times 10^{-6} \text{ s}^{-1}$ , and temperatures of 200, 288 and 400 °C. The DSA behaviour of the AISI 316NG stainless steel was additionally investigated at 150, 500, 600 and 700 °C. The strain rate sensitivity was measured using step-wise changes of the strain rate during tensile testing. Changes in the strain rate were performed both to the faster and the slower direction, i.e., with the ratio of initial and final strain rate ( $\dot{\epsilon}_1/\dot{\epsilon}_2$ ) equal to 10 and 100 or 0.1 and 0.01. These tests were performed at 200, 288 and 400 °C. To calculate the strain rate sensitivities in true stress – true strain coordinates a linear interpolation of each strain rate interval was performed.

Internal friction method was used in the study for evaluation of the free nitrogen content and its diffusion redistribution in the crystalline lattice of the studied stainless steels. Details of the test parameters are given in [7, 8].

Crack growth rate tests in simulated BWR NWC environment ( $\text{DO}_{\text{out}}$  500 ppb,  $\kappa_{\text{in}} < 0.1 \mu\text{S}/\text{cm}$ , T 290 °C, p 92 bar) were performed using rising and constant displacement loading and  $10 \times 10 \times 55 \text{ mm}^3$  SEN(B) specimens. Six specimens, five made of AISI 316NG stainless steel and one of sensitised AISI 304 (1050 °C/20 min + 680 °C/1 h + 500 °C/24 h) stainless steel were tested in the same autoclave equipped with bellow-loading devices. The AISI 316NG stainless steel was tested in non-deformed (one specimen), and deformed conditions (two specimens with 5% and two with 20% deformation). The sensitised AISI 304 stainless steel, used as a reference specimen to enable comparison of the test results with literature data, was tested in non-deformed condition. The tests were started with a displacement rate of  $5.5 \times 10^{-8} \text{ mm}/\text{s}$ , which was reduced to  $5.5 \times 10^{-9} \text{ mm}/\text{s}$ , when stable crack growth was detected and further to constant displacement loading condition after about 600 h testing time. The total testing time was 1198 h. The crack growth was

continuously monitored using the DC-PD technique. After the tests, the cracks were opened by fatigue, the final crack lengths were measured and the cracking morphology was determined using SEM.

## Results

The microstructure of all materials was austenitic. The grain size of the model alloys was smaller than that of the commercial AISI 316NG stainless steel, Table II. The slope of the increase in hardness was similar for all alloys, Figure 1.

Table II. Grain sizes and hardness of the studied materials.

Material and code	Grain size ASTM No / $\mu\text{m}$	Hardness [HV 10]		
		0% def.	5% def.	20% def.
AISI 316L, 1042	7 / 36	136	172	229
AISI 316L, 1043	6.5 / 43	159	191	255
AISI 316L, 1045	8 / 25	179	215	284
AISI 316NG, BB44	5 / 72	147	174	227
AISI 304, 165	4 / 101	nd	nd	nd

nd = not determined

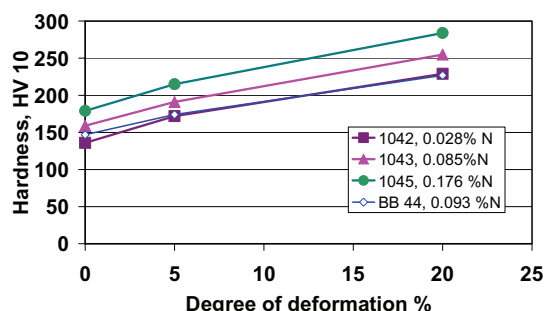


Figure 1. Hardness versus degree of deformation for AISI 316L stainless steels.

The mechanical properties are summarised in Table III. Nitrogen alloying increases the strength properties of AISI 316L stainless steels in the temperature range of 200 – 400 °C. The elongation to fracture ( $A_f$ ) decreases with increasing nitrogen content except for the commercial AISI 316NG stainless steel, which demonstrates the highest elongation to fracture in the whole temperature range of testing. The elongation to fracture varies only slightly as a function of temperature. The strain hardening coefficient ( $n$ ) increases with increasing testing temperature and decreasing nitrogen content. Yield strength ( $R_{p0.2}$ ) decreases with testing temperature, while tensile strength ( $R_m$ ) is almost constant in the studied temperature range.

Serrated yielding was observed in all AISI 316L stainless steels at testing temperatures above 200 °C and strain rates slower than  $10^{-4} \text{ s}^{-1}$ . At 200 °C serrated yielding appeared only for the material with the lowest nitrogen content of 0.028 %. For the AISI 316NG

stainless steel, tested in a wider temperature range, serrated yielding was observed at 288, 400 and 500 °C, but at lower (200 °C) and higher (600 and 700 °C) temperatures, serrated yielding disappeared, Figure 2.

Table III. Temperature dependencies of mechanical properties.

Material/ Code/ N-content (%)	T °C	R <sub>p0.2</sub> MPa	R <sub>m</sub> MPa	A <sub>t</sub> %	n
316L/ 1042/ 0.036	200	149	459	45	0.59
	288	143	465	49	0.62
	400	128	479	48	0.64
316L/ 1043/ 0.085	200	171	480	46	0.60
	288	143	477	47	0.62
	400	133	468	46	0.65
316L/ 1045/ 0.176	200	220	535	40	0.50
	288	198	539	42	0.58
	400	180	533	44	0.58
316NG/ BB44/ 0.093	200	181	470	52	0.52
	288	149	469	50	0.60
	400	141	472	49	0.61

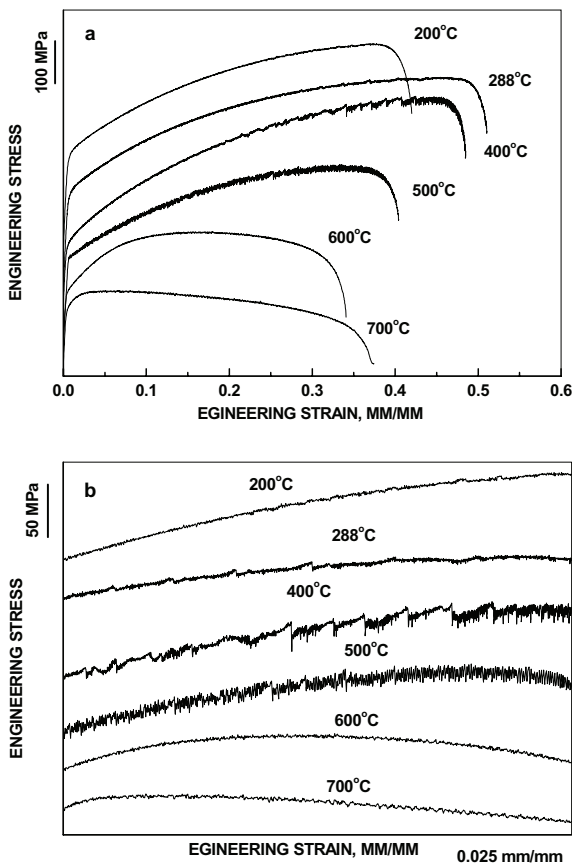


Figure 2. Engineering stress-strain curves obtained at strain rate of  $10^{-5} \text{ s}^{-1}$  in the temperature range of 200-700 °C (a) and magnified parts of the curves (b) for the AISI 316NG stainless steel with 0.093 % nitrogen.

The obtained stress-strain curves indicate that nitrogen alloying suppresses the DSA development in AISI 316L type stainless steels. Further, the amplitude of the stress pulses decreases markedly with the increase of nitrogen content and only a few pulses are present on the stress-strain curves of the stainless steels with 0.093 and 0.176 wt. % of nitrogen at testing temperature of 288 °C. A similar effect of nitrogen on DSA in AISI 316LN stainless steels was obtained in [6] at higher strain rates of testing.

Deformation by pre-straining at room temperature leads not only to an increase of yield and ultimate tensile strengths, but it reduces also the onset deformation of DSA, Figure 3. Serrated yielding can be observed on the stress-strain curve of AISI 316NG stainless steel obtained at testing temperature of 200 °C after 5 % pre-straining, Figure 4, but not in the solution annealed condition at this temperature. The results show that deformation facilitates the development of DSA in nitrogen-alloyed austenitic stainless steels.

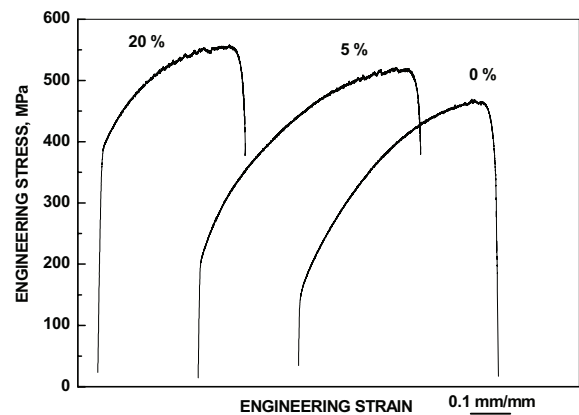


Figure 3. Engineering stress-strain curves obtained at 288 °C and strain rate of  $10^{-5} \text{ s}^{-1}$  for pre-strained AISI 316NG stainless steel.

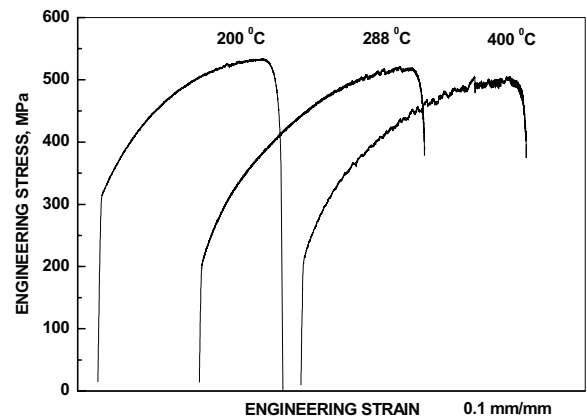


Figure 4. Engineering stress-strain curves obtained at strain rate of  $10^{-5} \text{ s}^{-1}$  for 5% pre-strained AISI 316NG stainless steel.

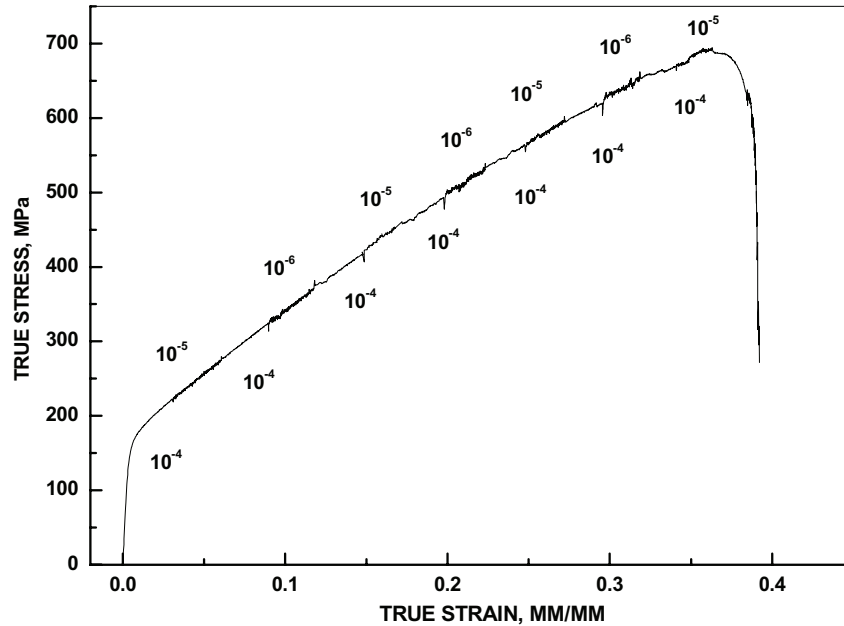


Figure 5. An example of true stress - true strain curve of AISI 316NG austenitic stainless steel obtained at 288 °C with step-wise strain rate changes equal to 10 and 100 or 0.1 and 0.01, respectively.

Changing the strain rate in steps during tensile loading results in clear changes in the serrated yielding, Figure 5, with more pronounced serrated yielding at lower strain rates.

The dependence between strain rate sensitivity and flow stress can be described by a linear approximation [9]. Close to the DSA region ‘anomalous’ behaviour is observed, which corresponds to a linear decrease of  $\Delta\sigma / (\Delta \ln \dot{\epsilon})$  with increasing flow stress. It can be seen from Figure 6 that the strain rate sensitivity decreases with increasing flow stress (i.e., increasing deformation) at all studied temperatures. Linear fitting to the data reveals positive strain rate sensitivity at 200 °C, values around zero at 288 °C and a clearly negative strain rate dependency at 400 °C. The results revealed a marked increase in the scatter of the data with increasing strain due to the localization of plastic deformation. Negative strain rate sensitivity of austenitic stainless steels corresponds to deformation under DSA conditions [3, 4]. As can be seen from Figures 6 and 2b, positive strain rate sensitivity value corresponds to deformation conditions where only minor serrations are observed on stress-strain curves at high values of flow stress. At 288 °C DSA serrations appear on the stress-strain curves only after certain amount of deformation, which corresponds to the observed change of positive strain rate sensitivity values to negative. At 400 °C, DSA serrations appear just after onset of plastic flow. The strain rate sensitivity remains negative in the whole strain range and at high values of flow stress the linear dependence is disturbed due to localisation of plastic deformation.

Type A serrations [3], observed in the performed investigations, correspond to quasi-regular separate pulses of flow stress. For evaluation of the average time between the pulses, the obtained stress-strain curves were transformed to frequency dependency

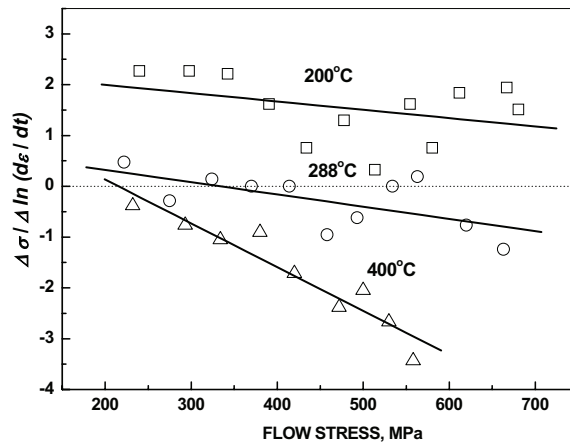


Figure 6. Dependence of strain rate sensitivity of AISI 316NG stainless steel on flow stress at temperatures 200, 288 and 400 °C.

using Fourier analysis [7, 8]. The Fourier analysis revealed that the time between the pulses is about 2.3 ks.

Internal friction (IF) of the studied stainless steels was mainly measured to check the presence of interstitial nitrogen atoms in the crystalline lattice of the studied stainless steels. Two IF peaks were observed, Figure 7, situated at about -50 °C and 100 °C. Both peaks increase with amount of cold deformation. These peaks represent presumably an inelastic response of dislocations interacting with point defects produced in the austenite crystalline lattice by cold deformation [10].

It is well established [11] that IF peak in the vicinity of 350 °C is caused by a Snoek-like relaxation process due to elemental diffusion jumps of interstitial nitrogen atoms in FCC crystalline lattice of austenite. The amplitude of the Snoek peak is proportional to the free nitrogen concentration. Thus, Figure 7 reveals that free nitrogen atoms are present in the AISI 316NG stainless steel at 288 °C. The concentration of the free nitrogen atoms in the lattice increases with the amount of pre-straining, in line with the tensile test results showing an earlier onset of DSA in deformed materials.

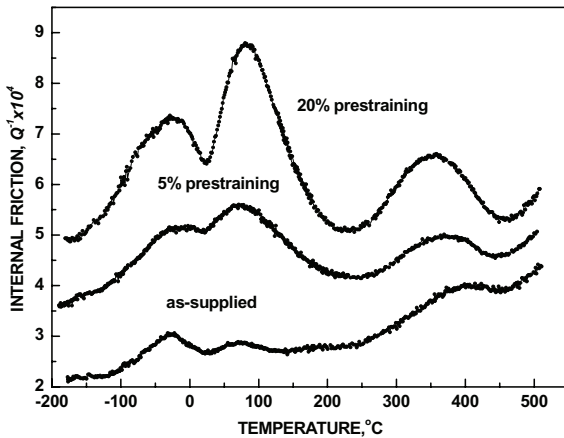


Figure 7. Temperature dependencies of internal friction for AISI 316NG stainless steel in as-supplied state (solution annealed) and after 5 % and 20 % pre-straining.

The observed increase of the nitrogen Snoek-like peak amplitude in the pre-strained stainless steel is reduced with ageing time at elevated temperatures, Figure 8, due to escape of free nitrogen from the solid solution. The peak reduction process can be described as a sum of three exponential decay functions (shown by dotted lines in Figure 8) with characteristic decay times of 0.6, 2.6 and 14.2 ks. The origin of the fastest component of the process is still unclear, while the second and third ones can be related to long-range diffusion escape of nitrogen from solid solution to dislocations and, probably, to grain boundaries. Ageing also results in an increase of the normalised shear modulus, indicating pinning of dislocations by nitrogen atoms due to ageing [5, 7].

The characteristic decay time of 2.6 ks, which represents the long-range diffusion of nitrogen to dislocations, is close to the value of the average time between serration pulses obtained from the stress-strain curves by Fourier analysis (2.7 ks). It seems that the repeated pinning of dislocations by diffusion of mobile nitrogen atoms, which is related to the advancement of Lüders bands, is a key element of DSA in AISI 316L stainless steels at testing temperatures used in this study.

In the crack growth rate tests in simulated BWR NWC environment, fully intergranular cracking was obtained in the sensitised AISI 304 stainless steel specimen and in one of the two 20% pre-strained AISI 316NG stainless steel specimens. Some IG

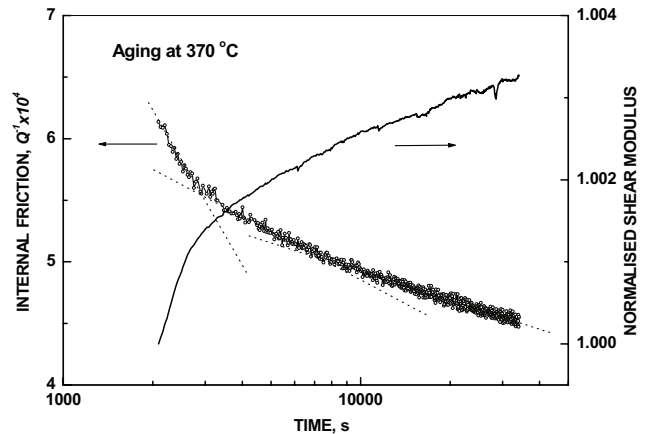
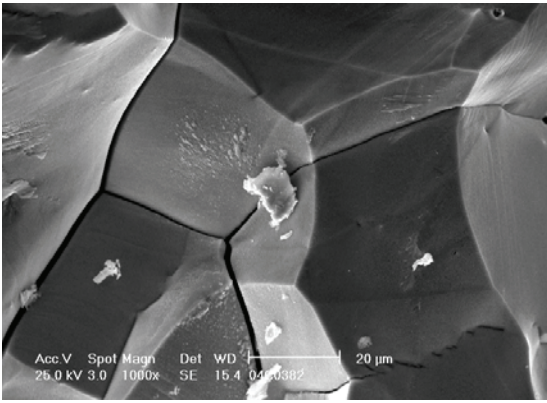


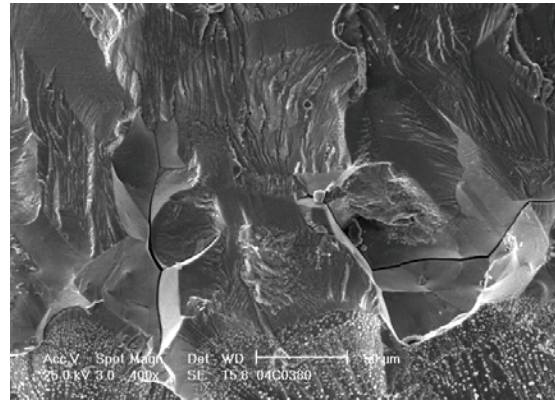
Figure 8. Amplitude of the Snoek-like peak of nitrogen and normalised shear modulus of AISI 316NG stainless steel as a function of ageing time at 370 °C. The dotted lines represent the three components of the peak amplitude decay.

fracture was also observed in one of the two 5% pre-strained AISI 316NG stainless steel specimens, Figure 9. All other specimens revealed mainly transgranular cracking. The crack growth rates obtained for the sensitised AISI 304 stainless steel are in the order of  $10^{-7}$  mm/s and similar to those obtained using  $10 \times 10 \times 55$  mm<sup>3</sup> SEN(B) and 25 mm C(T) specimens in reference [12], Figure 10a. The crack growth rates of sensitised AISI 304 stainless steel depend on the loading mode: the crack growth rates are lower by a factor of 2 to 10 under constant displacement than under rising displacement conditions. All crack growth rates are also plotted as a function of loading rate, in terms of J-integral increase rate  $dJ/dt$ , in Figure 10b.  $dJ/dt$  is a measure of loading rate independent of the specimen size and loading geometry [12].

The results revealed a higher tendency for the 20% deformed AISI 316NG stainless steel to intergranular environmentally assisted cracking (EAC) in BWR NWC environment compared to non-deformed, non-sensitised stainless steel. However, the susceptibility to EAC is much lower than that in sensitised stainless steels, in accordance with expectations. The crack growth rate at a similar loading rate (i.e.,  $dJ/dt$ ) is one order of magnitude higher in the sensitised AISI 304 stainless steel compared to that in 20% deformed AISI 316NG stainless steel. The crack growth rate in 5% deformed AISI 316NG stainless steel showing mixed transgranular and intergranular cracking was in the same order as in the sensitised AISI 304 stainless steel. However, there was a ripple loading fatigue component of  $R \sim 0.9$  and  $f \sim 1$  Hz present during that test, which can be expected to result in partially transgranular fracture morphology and also in enhanced crack growth rate.

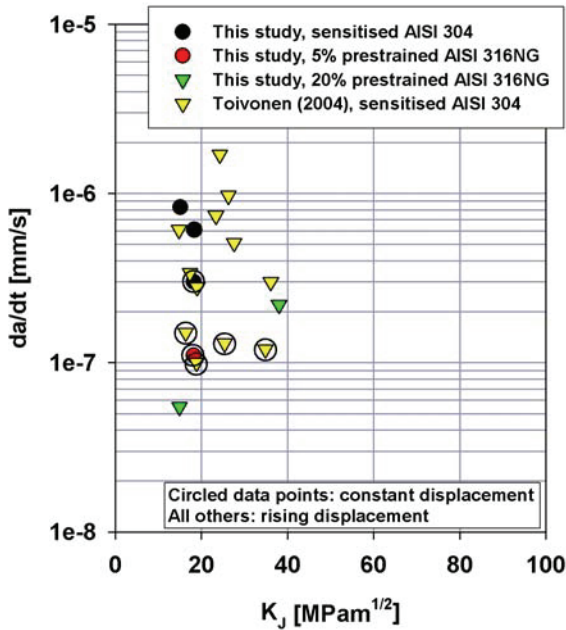


(a)

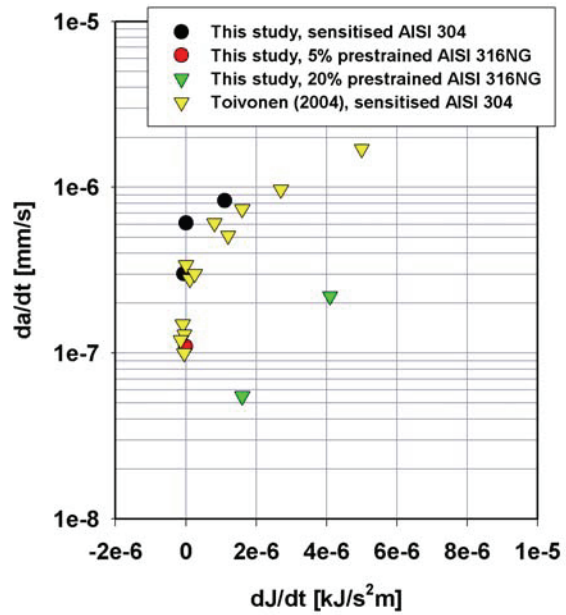


(b)

Figure 9. Fractographs showing fully intergranular cracking in the specimen made of 20% pre-strained AISI 316NG stainless steel (a), and mixed transgranular and intergranular cracking in the specimen made of 5% pre-strained AISI 316NG stainless steel (b) after constant displacement testing in BWR NWC environment.



(a)



(b)

Figure 10. Crack growth rate as a function of  $K_I$  for the crack growth rate tests with observed intergranular cracking (a) and as a function of the loading rate in terms of  $dJ/dt$  (b). A fatigue component of  $R \sim 0.9$  and  $f \sim 1$  Hz was present during the constant displacement phase of the test with the specimen made of 5% pre-strained AISI 316NG stainless steel.

### Discussion

The results obtained in the present investigation are in good accordance with literature data on nitrogen effects on DSA in AISI 316L stainless steels. Serrated yielding within temperature range of about 200 – 500 °C manifested DSA in the investigated stainless steels. The DSA behaviour was dependent on the nitrogen content and degree of pre-straining. Strain rate sensitivity investigations revealed further a negative strain rate sensitivity for the AISI 316NG stainless steel, which is a clear evidence of DSA behaviour. A map of DSA, shown in Figure 11, summarises the

serrated flow appearance in AISI 316NG stainless steel at different strain rates and testing temperatures. The dashed line in Figure 11 forming a boundary for testing parameters, where DSA occurs, extends to lower strain rates applied in the present investigation as compared to those in [6].

The enthalpy calculated using the dashed line in Figure 11 is about 1.24 eV and its value is very close to the enthalpy of nitrogen diffusion calculated from the Snoek-like internal friction peak, 1.45 eV at 350 °C [7, 8].

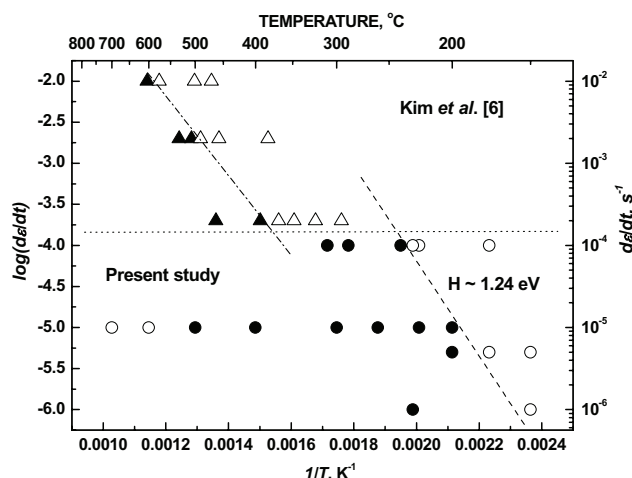


Figure 11. Map of DSA serration occurrence as a function of strain rate and temperature of AISI 316NG stainless steel. Filled symbols correspond to strain rate and temperature values at which DSA (serrated yielding) was observed on stress-strain curves. Data points shown by triangles above the dotted line were obtained in [6]. The dashed lines are the boundaries for the DSA appearance in this study and in [6].

The obtained strain hardening coefficient values are high, especially for the elevated testing temperatures, where DSA serrations are remarkable. In fact, in these conditions, the stress-strain curves do not follow the Holomon law in the whole plastic strain range. The strain hardening coefficient is highest for the stainless steel with the lowest nitrogen content, in which the DSA serrations are most pronounced.

The DSA results showing that nitrogen alloying suppresses the onset strain and temperature range of DSA indicate that nitrogen alloying may also lower the EAC susceptibility, if DSA is considered to be a part of the decisive mechanism. The crack growth rate test results obtained in this study are in line with literature and field experience showing increased susceptibility and increased crack growth rates in the non-sensitised stainless steels due to deformation [13]. However, the crack growth rates in deformed, non-sensitised stainless steels are much lower than those in sensitised stainless steels in BWR NWC environment. Crack growth rate tests on stainless steels have revealed a correlation between susceptibility to intergranular cracking, CGR and yield strength [13]. The yield strength increases as a function of deformation, but also as a function of nitrogen content. As these materials are non-sensitised, corrosion must be less decisive and localisation of plastic deformation to the grain boundaries is more important than in the case of sensitised stainless steels. More CGR tests are needed in order to determine the EAC crack growth rates of non-sensitised stainless steels as a function of deformation and chemical composition.

A suppression of the DSA development in the studied stainless steels caused by nitrogen alloying looks contradictory as DSA, e.g. in low alloy steels, is enhanced by free interstitials. The suppressive effect of nitrogen on DSA may be caused by the increase of the flow stress with nitrogen alloying of the stainless steel causing an increase of the actual stress and consequent changes in the deformation response. DSA is expected to result in

localisation of plastic deformation to grain boundary regions. This is also the case in deformed materials, where DSA was observed at all studied nitrogen levels. A detailed mechanism of the role of DSA in EAC and the role of deformation as well as stainless steel composition needs further investigations to reveal the main parameters affecting EAC in deformed, non-sensitised stainless steels in high temperature water such as BWR NWC.

## Conclusions

- DSA in nitrogen-alloyed AISI 316L type stainless steels can occur at temperatures above 200 °C at strain rates slower than  $10^{-4} \text{ s}^{-1}$ .
- DSA is manifested by serrated yielding, negative strain rate sensitivity and IF peaks.
- Nitrogen suppresses the DSA development in AISI 316L type stainless steels. The onset deformation of DSA serrations shifts to higher values of strain and the amplitude of the flow stress pulses decreases with increasing nitrogen content.
- Pre-straining at room temperature decreases the onset temperature and strain of DSA in AISI 316NG stainless steel.
- An apparent activation enthalpy of DSA in AISI 316NG stainless steel is about 1.24 eV at temperatures around 300 °C. The value of enthalpy of DSA corresponds well to the enthalpy of nitrogen diffusion in AISI 316NG stainless steel, about 1.45 eV, obtained by the internal friction method.
- Pre-straining increases the susceptibility of non-sensitised AISI 316NG stainless steel to intergranular stress corrosion cracking in BWR NWC environment. The crack growth rate is, however, lower than that for sensitised stainless steel.

## Acknowledgements

This presentation is prepared within the project Structural operability and plant life management (RKK, XVO and INTEL), which is coordinated by Teollisuuden Voima Oy. The work has been funded by the National Technology Agency (Tekes), Teollisuuden Voima Oy (TVO), Fortum Power and Heat Oy, Fortum Nuclear Services Ltd., FEMdata Oy, Neste Engineering Oy, Fortum Oil and Gas Ltd. and VTT. The Swedish Nuclear Power Inspectorate, SKI, participated also in this work. Their funding is gratefully acknowledged.

## References

1. U. Ehrnstén, P. Aaltonen, P. Nenonen, H. Hänninen, C. Jansson, T. Angelii. "Intergranular Cracking of AISI 316NG Stainless Steel in BWR Environment," *Proc. of 10<sup>th</sup> International Conference on Environmental Degradation of Materials in Nuclear Power Systems - Water Reactors, Nevada, USA, 5 - 9 August (2001)*, ANS; NACE; TMS (2001), 10 p.
2. T. Angelii. "Microstructural Characterization of L-Grade Stainless Steels Relative to the IGSCC Behavior in BWR Environments," *Proc. of Corrosion 2001. NACE, Houston, Texas, March 11-16 (2001)*, Paper No 01121, 14 p.

3. L. H. de Almeida, I. LeMay, P. R. O. Emygdio, "Mechanistic Modeling of Dynamic Strain Aging in Austenitic Stainless Steels," *Mater. Characterization*, 40 (1998), 137 - 150.
4. L.H. de Almeida, P.R.O. Emygdio, "Activation Energy Calculation and Dynamic Strain Aging in Austenitic Stainless Steel," *Scr. Met. et Mater.*, 31 (1994), 505-510
5. R. Ilola, M. Kemppainen, H. Hänninen, "Dynamic Strain Ageing of Austenitic High Nitrogen Cr-Ni and Cr-Mn Steels," *Proc. of 5<sup>th</sup> Int. Conf. "High Nitrogen Steels '98"*, *Mat. Sci. Forum*, 318-320 (1999), 407 - 412.
6. D.W. Kim, W.-S. Ryu, J.H. Hong, S.-K. Choi, "Effect of Nitrogen on the Dynamic Strain Aging Behaviour of Type 316L Stainless Steel," *J. Mater. Sci.*, 33 (1998), 675-679.
7. M. Ivanchenko, U. Ehrnstén, V. Nevadacha, Y. Yagodzinskyy and H. Hänninen, "Dynamic Strain Ageing of Nitrogen-Alloyed AISI 316L Stainless Steel," *Proc. of the 7<sup>th</sup> Int. Conf. "High Nitrogen Steels 2004"*, *Ostend, Belgium, September 19-22 (2004)*, 641 - 649.
8. U. Ehrnstén, M. Ivanchenko, V. Nevadacha, Y. Yagodzinskyy, A. Toivonen, H. Hänninen, "Dynamic Strain Ageing of Nitrogen-alloyed AISI 316L Stainless Steel," *Proc. of Eurocorr 2004, Nice, France, 13-16.9 (2004)*, Event No. 226. 10 p.
9. R.A. Mulford and U.F. Kocks, "New Observations on the Mechanisms of Dynamic Strain Aging and of Jerky Flow," *Acta Metallurgica*, 27 (1979), 1125-1134.
10. C.F. Burdett, T.J. Queen, "Role of Dislocation in Damping," *Met. Rev. (Suppl. to Metals Mater.)*, 15 (1970), 47 - 65.
11. Yu. Jagodzinski, S. Smouk, A. Tarasenko, H. Hänninen, "Distribution of Interstitial Impurities and their Diffusion Parameters in High-Nitrogen Steels Studied by Means of Internal Friction," *Proc. of 5<sup>th</sup> Int. Conf. "High Nitrogen Steels '98"*, *Mat. Sci. Forum*, 318-320 (1999), 47 - 52.
12. A. Toivonen, "Stress Corrosion Crack Growth Rate Measurement in High Temperature Water using Small Pre-cracked Bend Specimens," *VTT Publications 531 (2004)*, 206 p. + App.
13. P. Andresen, P. Emigh, M. Morra, R. Horn, "Effects of Yield Strength, Corrosion Potential, Stress Intensity Factor, Silicon and Grain Boundary Character on the SCC of Stainless Steels," *Proc. of 11<sup>th</sup> Symposium on Environmental Degradation of Materials in Nuclear Power Systems – Water Reactors, Stevenson, WA, August 10-14 (2003)*, 816-833.